

A Physical Modeling Study on the Dynamic Response of Flexible Retaining Walls with Deformable EPS inclusion



O.L. Ertugrul

Mersin University, Dept. Of Civil Engineering, Mersin, Turkey

A. C. Trandafir

Fugro GeoConsulting, Inc., Houston, Texas, USA

SUMMARY

Recent research demonstrated that expanded polystyrene (EPS) geofoam can be utilized as an efficient deformable inclusion to reduce the seismic earth pressures against rigid non-yielding retaining walls. In the light of previous studies, the present investigation explores the potential application of EPS geofoam seismic buffers in reducing the dynamic earth pressures and lateral deflections of flexible cantilever retaining walls during earthquake. Results of 1-g physical model tests addressing the dynamic behavior of yielding cantilever retaining walls with EPS geofoam compressible buffers are discussed. The effect of relative flexibility of the wall as well as the thickness of the compressible buffer was investigated in this context. The dynamic response of the retaining wall model was evaluated in terms of flexural wall deflections and lateral earth pressures within the backfill. Dynamic earth pressure coefficients were calculated from the lateral stresses measured in the physical tests and compared with those calculated using methods available in the literature. It was observed that an increase in the relative wall flexibility provides reduction in the dynamic earth pressure coefficients. The presence of an EPS geofoam buffer provides additional reduction in dynamic earth pressure coefficients for the investigated relative wall flexibility range. Predictions obtained by the analytical methods are in better agreement with the results from physical model tests for wall models having lower relative flexibility values.

Keywords: EPS geofoam, yielding retaining wall, wall flexibility, 1-g physical test

1. INTRODUCTION

Years of practical experience with polymeric geofoam proved its ability to withstand vertical and lateral stresses when used in the construction of earthworks. The stability, durability, and resistance to moisture and deterioration are the superior properties of rigid cellular geofoam. Since the bulk density of the geofoam can be adjusted according to the diverse range of applications, geofoam replaced all the previous materials used as compressible inclusion or lightweight fills. Geofoam products have also been used as a countermeasure for earthquake induced displacements on retaining structures, buried pipelines and underground structures. For seismic applications, elasticized geofoam products have a better ability to attenuate earthquake forces since the elastic portion of this type of geofoam may reach up to 10% strain.

Most earth retaining structures are analyzed and designed based on the assumption that static active lateral earth pressure conditions exist in the retained backfill. Horvath (1997) indicated that this assumption is appropriate if the structure enables enough lateral deformation in the retained soil. In many cases, external restraints and inherent rigidity of the retaining wall prevents the wall movements required for the shear strain mobilization of the backfill. Recent research demonstrated that presence of deformable inclusions between the backfill and retaining structure successfully reduces static earth pressures on rigid non-yielding retaining walls (Ertugrul and Trandafir, 2012).

Influence of deformable buffers on the earth pressures developed against retaining walls under dynamic excitations has been investigated extensively by Bathurst (2007). 1-g shaking table tests were carried out on 1 m high rigid walls with EPS geofoam inclusions. Performance of the deformable

inclusion was evaluated for different loading conditions, backfill and inclusion assortments. Harmonic base excitations were applied to the base of the wall-backfill model. Results showed that reductions up to 40% may be achieved for the seismic thrust at the peak excitation amplitude of 0.7g. The initial elastic tangent modulus of the deformable material played the major role in reduction of lateral forces.

Athanasopoulos et al. (2007) performed numerical modeling studies for EPS seismic buffers. The flexibility of the retaining wall on the performance of buffers was investigated. It was reported that increasing flexibility of the wall has a positive role on the isolation efficiency (the ratio of change in the wall force for seismic buffer case divided by peak wall force without buffer). Five different geofoam materials having densities in the range of 1.3 kg/m³ to 16 kg/m³ were placed as deformable buffer between granular backfill and rigid retaining wall model. Dynamic load attenuation of the deformable buffers decreased as the peak amplitude of the excitation increased. It was reported that isolation efficiency decreases significantly for excitation frequencies in the vicinity of the fundamental frequency of the backfill-buffer-retaining structure.

Zarnani and Bathurst (2009) carried out a numerical modeling study using FLAC finite difference code. Lateral dynamic earth thrust and compressive buffer strains were calculated for rigid walls subjected to various earthquake records. Influence of wall height and EPS geofoam characteristics were investigated throughout a parametric study. Significant decrease in the seismic loads on the wall was observed in the presence of vertical deformable buffers made of EPS geofoam. A slightly larger reduction in the lateral load with increasing thickness of the deformable buffer was also noticed. The stiffness of the deformable material played an important role in load reduction efficiency which is also observed in the static counterpart of the load reduction concept by compressible buffers.

The dynamic interaction mechanism of the backfill-deformable inclusion and retaining structure requires further investigation. The use of experimental modeling provides valuable insight on clarifying this problem. In the current study, the influence of expanded polystyrene geofoam panels of low stiffness installed vertically against yielding retaining walls was investigated through dynamic physical model tests. Results of small-scale shaking table tests on model retaining walls with deformable EPS geofoam inclusions were interpreted and discussed in this context. Model walls having various flexibility ratios were instrumented with pressure, displacement and acceleration transducers. Results of model tests were compared to those of previous experimental work. Back-calculated dynamic earth pressure coefficients were compared to those obtained from Mononobe-Okabe and Steedman-Zeng methods.

2. METHODOLOGY

The physical modeling study focuses on the dynamic response of cantilever earth retaining wall models with compressible geofoam buffers placed between the wall and the cohesionless granular backfill. In the tests, wall displacements, lateral dynamic earth pressures along the wall height, accelerations within the backfill were monitored under harmonic base excitations. Tests were performed in a laminar container with dimensions of 1.5m×1m×1m placed on a uni-axial shaking table. A perspective view of the test set-up is depicted in Fig.1. Excitation system was capable of generating harmonic displacements up to 1.2g acceleration amplitude within 1Hz -11 Hz frequency range. Data acquisition system is composed of acquisition card with 12 bit resolution for 16 input channels, signal conditioning units and transducers. The influence of the inertial, frictional and membrane stiffness effects of the laminar container were investigated and the outputs regarding the accelerations were adjusted to decrease the influence of these factors.

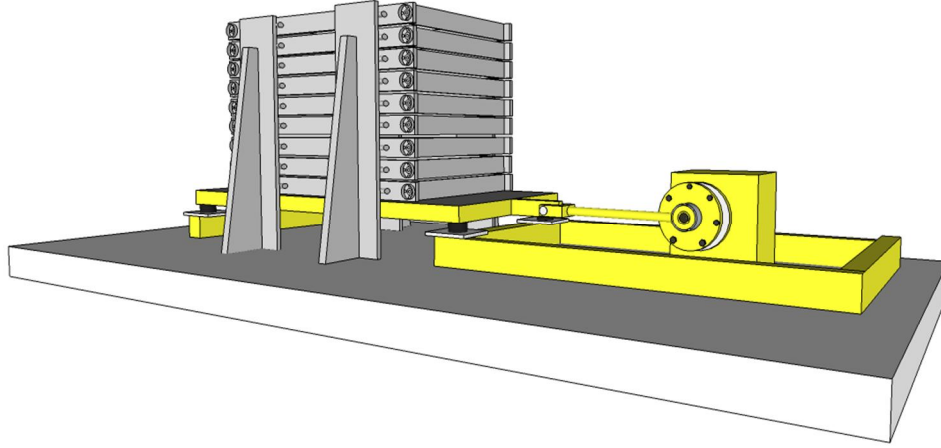


Figure 1. Perspective view of the laminar container and the excitation system

2.1. Characterization of the granular backfill material used in the physical model tests

Various index properties of the material are summarized in Table 2.1. The grain size distribution of the granular backfill material was determined by dry sieving procedure. The model sand has 1.15% fines (silt and clay). C_c and C_u was determined as 0.80 and 3.31, respectively. According to the Unified Classification system, material was classified as poorly graded sand (*SP*). Maximum and minimum void ratios of the soil were determined as 0.745 and 0.436, respectively. Specific gravity (G_s) was determined as 2.66 in accordance with ASTM D854-83 testing procedures. Isotropic consolidated-drained (CD) tests were performed on samples having a relative density of 70%. Based on CD test results, internal friction angle of the material was determined as 43.5° . The dilatancy angle of the sand was determined as 22.5° from volumetric strain measurements. The relatively high value of dilation angle was associated with the low confining stresses applied in the triaxial tests. Secant modulus (E_{50}) of the granular cohesionless material is determined as 5200 kPa from stress-strain curve derived from triaxial test data. Stress controlled cyclic triaxial tests were performed on the samples to determine the dynamic modulus of elasticity and damping ratio of the granular material. In all of the cyclic tests, cyclic component of the stress remained below the static confining stresses; hence the specimen was always subject to compression. Samples having relative density (R_d) of 70% were tested by applying the static confining stress first and proceeding with the cyclic component of the stress. Tests were repeated for various cyclic deviator stresses. Average secant shear modulus (G_{sec}) was determined as 7200 kPa and damping ratio (ζ) as 2.88% for the confining stress range of the physical model tests. The small-strain dynamic modulus value of the model sand in this study was calculated by the following empirical formula for angular grained sands (Chang and Makarechi, 1982):

$$G_{max} = 1230 \frac{(2.973 - e)^2}{1 + e} \sigma_m^{0.5} \quad 2.11$$

where e is the void ratio and σ_m is the confining stress. The G_{max} value for $e=0.523$ is determined as 11650 kPa with Eq.2.1.

2.2. Characterization of the low stiffness EPS used in the physical model tests

The density of the EPS material chosen for the tests was determined as 15.2kg/m^3 . According to ASTM Standard C578-05, EPS geof foam used in the tests was classified as TYPE I. The Young's modulus (E_{av}) of the linear elastic range of the material and yield stress (σ_y) is found as 1500 kPa and 38 kPa, respectively, from uniaxial compression testing of the EPS-15 geof foam. The uniaxial monotonic loading test was carried out at an axial strain rate of 0.01% strain/min that is consistent with the loading rate of the EPS geof foam panel during the backfilling process of the 700 mm high

retaining wall model. Static consolidated-undrained type triaxial tests were performed on cylindrical EPS samples under three different confining stresses and results were depicted in Fig.2. Results of uniaxial tests were considered to be more representative of the stress-strain behavior of the geofoam since confining stresses on the vertical deformable buffer are relatively low given the small height of the backfill. Initial tangent modulus (E_{ti}) and Poisson's ratio (ν) were calculated according to the following empirical relationships proposed by Horvath (1995):

$$E_{ti} = 0.45\rho - 3 \quad 2.22$$

$$\nu = 0.0056\rho + 0.0024 \quad 2.3$$

where E_{ti} is the initial tangent modulus in MPa, ρ is the density in kg/m^3 and ν is the Poisson's ratio. Using Eq. 2.2 and Eq.2.3, E_{ti} and ν are determined as 3750kPa and 0.086, respectively. Dynamic shear moduli and damping ratio of EPS-15 were determined based on the cyclic triaxial test data. Typical hysteresis loops under different cyclic deviator stresses were depicted in Fig. 3. The dynamic properties of EPS-15 determined from cyclic triaxial tests are depicted in Table 2.1. Due to lack of small-strain test data (resonant column test, bender element test etc.), the small-strain dynamic shear modulus (G_0) value and Poisson's ratio (ν_0) of the EPS-15 was estimated as 3400 kPa and 0.2695 using the following empirical formulas proposed by Athanasopoulos et al. (2007) based on resonant column test data:

$$\frac{G_{0(\sigma_3)}}{G_{0(\sigma_3=0)}} = 1.02 + 0.599 \frac{\sigma_3}{\sigma_c} - 1.41 \left(\frac{\sigma_3}{\sigma_c} \right) \quad 2.4$$

$$\nu_{0(\sigma_3)} = 0.25 - 0.33 \left(\frac{\sigma_3}{\sigma_c} \right) \quad 2.5$$

where σ_3 is the confining stress and σ_c is the compressive strength of EPS samples with $h:d$ ratio of 2. G_0 and ν_0 were estimated as 5231kPa and 0.212, respectively for $\sigma_3=15\text{kPa}$.

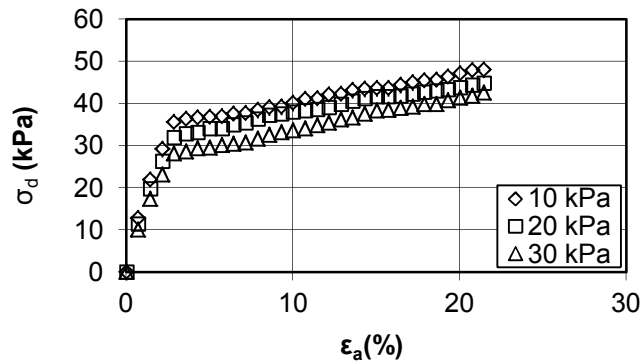


Figure 2. Monotonic stress-strain behavior of EPS-15 (strain rate 0.01%/min)

2.3. Physical modeling test program

In the first group (control tests), compressible buffer was not present between the retaining wall model and the backfill. In the second test set, deformable EPS-15 buffers of different thicknesses ($t/H=0.07$ and 0.14 , t is the inclusion thickness and H is the wall height) were installed between the model walls

and the backfill. The models were excited by harmonic displacements to match a target sinusoidal accelogram with various frequencies within a range of 4.25 Hz to 10 Hz. The amplitude of the accelogram varied from 0.06g to 0.7g. Gradually increasing and decreasing type excitations were applied at the beginning and the end of the base motion to prevent the impact type loading effect on the retaining wall models.

Table 2.1. Summary of cyclic triaxial tests on EPS-15

$(\sigma_d)_{cyclic}$ (kPa)	$(\varepsilon_d)_{max}$ (%)	ζ (%)	E_{sec} (kPa)	G_{sec} (kPa)
3	0.093725	2.549	3434	1533
6	0.15838	3.295	4429	1428
9	0.278915	4.211	2670	1191
12	0.3533	4.573	2532	1253
14	0.43225	5.185	2178	972

Application of a simple harmonic base excitation allows all of the retaining wall models to be excited in the same controlled way which enables more accurate comparisons to be made about the effect of variables investigated in this study. According to Bathurst and Hatami (1998), frequencies in the range of 2Hz-3Hz are considered as representative of predominant frequency content of medium to high frequency earthquakes. Based on the scaling relationships proposed by Iai (1989), base excitations having a frequency range between 5Hz and 10Hz at 1/10 model scale correspond to 1.58Hz and 3.16Hz in the prototype scale.

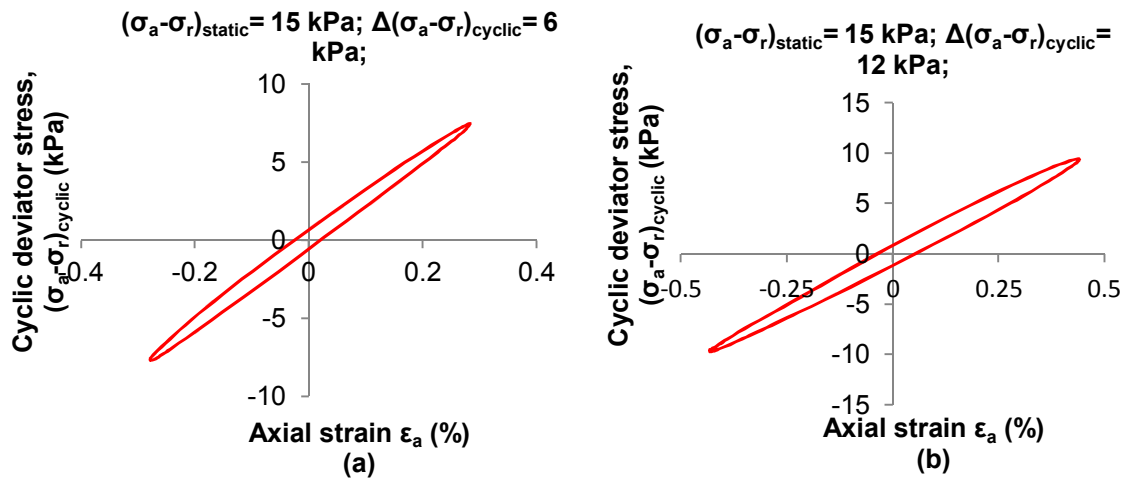


Figure 3 Typical hysteresis loops for EPS-15 ($f = 3.00\text{Hz}$; $N = 10$ cycles)

Tests were carried out on instrumented model walls and backfill. The model walls were comprised of steel with dimensions of 700×980×(2,4,5,8) (height×length×thickness in mm's) rigidly welded to a steel base of 980×500×8 (length×width×thickness in mm's). Displacements of the wall stem, lateral earth pressures, and acceleration magnitudes at various locations on the wall and in the backfill were monitored during the test series. Cross section of the model and the positions of the instruments were depicted in Fig. 4. Instrumented model walls were placed on 30 cm thick layer of vibro-compacted granular material. Backfill was formed with raining technique of the granular material to achieve relative density of approximately 70% as described by the procedure proposed by Okamoto (2006). Following the preparation of backfill, data acquisition system was activated to monitor wall pressures. During the backfilling stage, wall stem was kept fixed against lateral sliding. Prior to the data acquisition phase, horizontal fixity of the wall was slowly removed by unloading the mechanical jack located between the wall model and short side of the soil container. Wall pressures and deflections were measured until no further wall deflection and pressure redistribution occur. During the removal

of lateral fixity, sliding and rotation of the retaining wall were not observed. Hence, measured displacements were considered as pure flexural deflections of the wall model. Following the data acquisition for the static phase, the preparations for the dynamic phase started. Before the activation of the excitation generator, data acquisition started and data is collected for duration of 30 seconds to observe probable fluctuations in the initial readings of the transducers. Full amplitude base excitations were applied to the laminar container for duration of 7 seconds. Tests involving compressible geofoam inclusions were carried out by following the same procedure, however, deformable EPS inclusions were installed between the wall model and the backfill prior to the pluviation of backfill material.

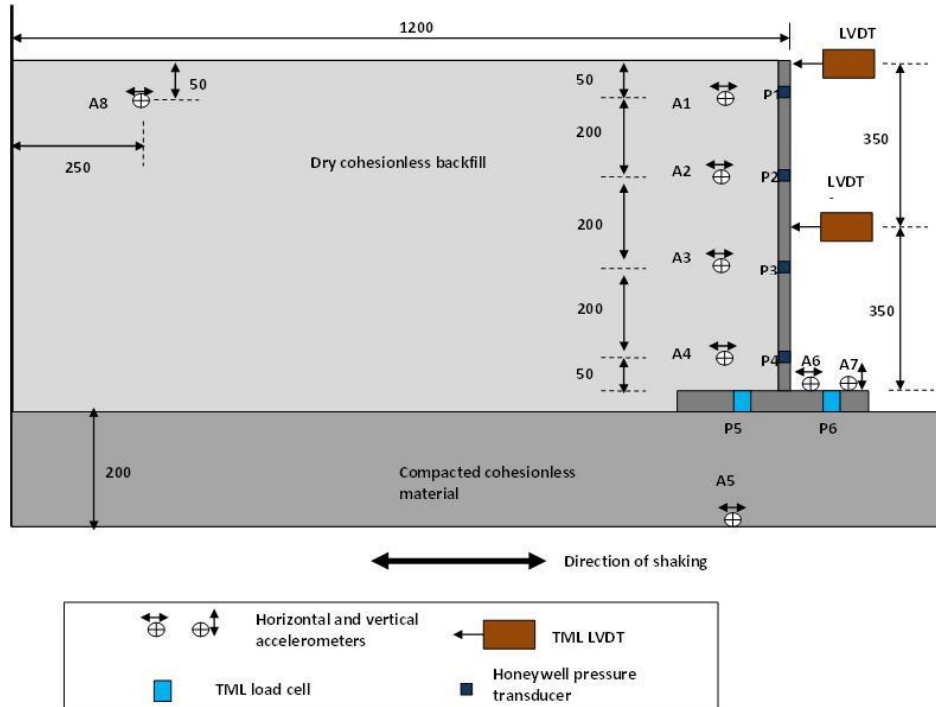


Figure 4 Locations of the transducers used in the physical models

3. RESULTS AND DISCUSSION

According to Younan and Veletsos (2000), relative flexibility (d_w) is considered as the primary parameter affecting the response of the system and defined as:

$$d_w = 12(1 - \nu_w^2) \frac{G}{E_w} \left(\frac{H}{t_w} \right) \quad 3.1$$

where G is the shear modulus of the backfill, H is the wall height, E_w is the Young's modulus of the wall, t_w is the wall thickness and ν_w denotes the Poisson's ratio of the wall material. According to Eq.3.1, d_w values were calculated as 128, 524, 1024 and 8197 for various wall stem thicknesses of model walls. Dynamic wall deflections at the wall tip were compared for different relative wall flexibility values under the applied base motion having amplitude of 0.3g at 4.25Hz frequency. The effect of wall flexibility on the wall deflections expressed as $(\delta_h)^{1/3}$, where δ_h is the lateral deflection measured at the top of the wall in m, were depicted in Fig. 5. Wall flexibility significantly affects the performance of the geofoam seismic buffers. An increasing trend was observed in flexural deflections when relative wall flexibility (d_w) increases. Decrease in flexural wall deflections for buffer thickness of $t/H=0.14$ may reach up to 20% for the most flexible model wall ($d_w=8197$). Evolution of the dynamic component of the total lateral thrust (P_{dyn}) for the most flexible wall ($d_w=8197$) and most rigid ($d_w=128$) model wall are compared in Fig.6 (a) and (b). For the same model walls with the presence of a compressible inclusion having t/H ratio of 0.07, the dynamic thrust time histories were depicted in

Fig. 7(a) and (b). It was observed that amplitude of dynamic thrust is significantly high for the least flexible wall ($d_w=128$). At the end of dynamic phase, a residual lateral force remained on the wall due to the densification of the soil during the excitation. The relative density of the backfill at the end of dynamic phase was observed to be in the range of 80% to 85%.

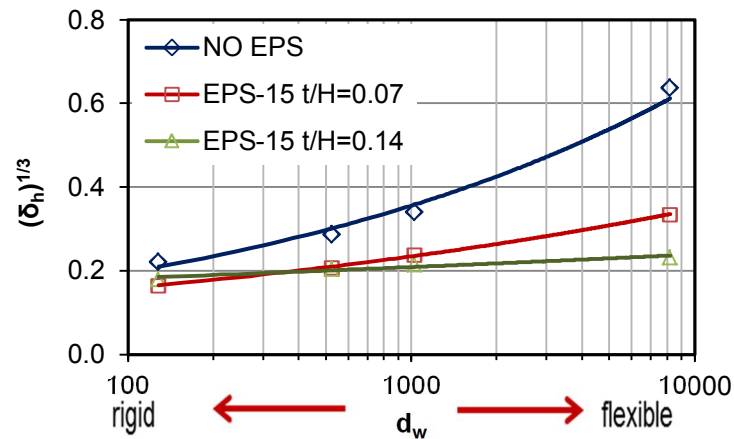


Figure 5 Flexural deflection (power of 1/3) versus d_w

Initial static stress profile and the total dynamic pressure distribution leading to peak dynamic thrust were depicted in Fig.8 (a) and (b). Active static pressure distribution calculated according to Coulomb theory was indicated on the same figures. There are significant variations in the pressure profiles of flexible and rigid model. Initial static pressures for the rigid model are significantly higher than those of the flexible one. Initial pressures for the flexible wall are observed to be close to the theoretical active pressure distribution whereas those for the rigid model were higher than the theoretical active distribution which indicated that deformations in the backfill are not large enough for the mobilization of the soil shear strength along the failure wedges. The dynamic pressures were significantly higher for the rigid model wall than those of the flexible one. In Fig. 9 (a) and (b), pressure profiles for the model walls with EPS deformable buffer ($t/H=0.07$) were depicted. The presence of deformable buffer provides decrease in both initial static and total dynamic earth pressures. Effect of relative wall flexibility (d_w) on the total lateral thrust (P_{ae}) and total base moments (M_{ae}) for the model walls with and without compressible geofoam inclusion is depicted in Fig.10 (a) and (b). The positive effect of the wall flexibility on the thrust and bending moment are clearly demonstrated in these figures. The contribution of the deformable buffers on the wall forces varies in relation to the relative wall flexibility and deformable buffer thickness. For a given wall stiffness, larger thicknesses of the EPS geofoam panel translate into greater reduction in the dynamic wall thrust and bending wall moment. An increase in the retaining wall stiffness is associated with a more pronounced effect of the geofoam buffer in reducing the dynamic earth forces.

Seismic lateral earth pressure coefficients $(K_{ae})_{exp}$ were back-calculated based on lateral stresses measured during physical tests. The lateral seismic earth pressure coefficients $(K_{ae})_{exp}$ are calculated by Eq.3-2:

$$(K_{ae})_{exp} = \frac{2}{\gamma H^2} \int_0^H \sigma_x dz \quad 3-2$$

where H is the wall height, γ is the backfill unit weight and σ_x is the lateral earth pressure (including static and dynamic component) at depth (z). A comparison of the lateral dynamic earth pressure coefficients obtained from physical tests and other methods were made in Fig.11. For the most stiff wall, dynamic coefficients are under predicted by available methods whereas for the least stiff type model, methods over predict the observed values. The contribution of the compressible buffers on the lateral dynamic earth force is generally observed to be more pronounced for stiffer walls however important amount of reduction was observed for the least stiff retaining wall model. Approximately 50% decrease was observed in $(K_{ae})_{exp}$ values by using an EPS geofoam buffer ($t/H=0.14$) for the wall

model with $d_w=128$. The same geofoam buffer provides 33% decrease in $(K_{ae})_{exp}$ for the wall model with $d_w=8197$.

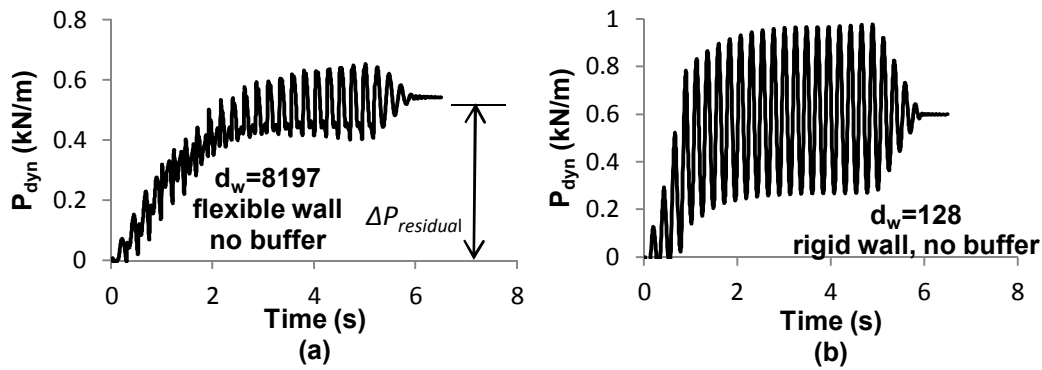


Figure 6 Evolution of the dynamic forces for the flexible and rigid model without deformable EPS inclusion

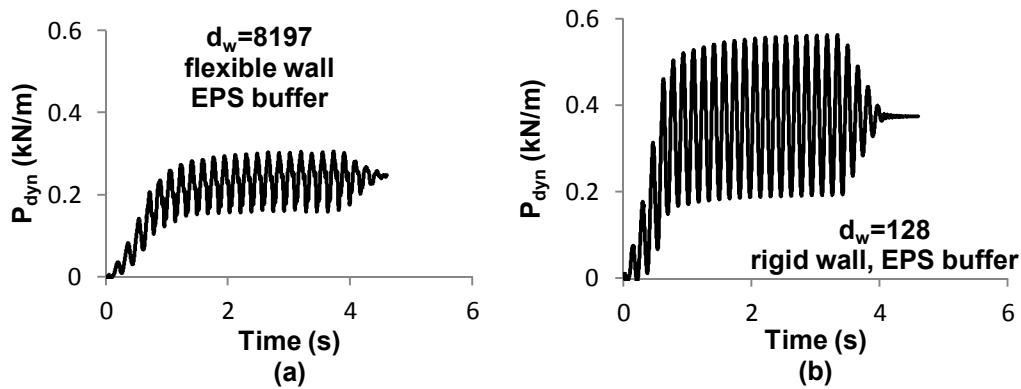


Figure 7 Evolution of the dynamic forces for the flexible and rigid model with deformable EPS inclusion

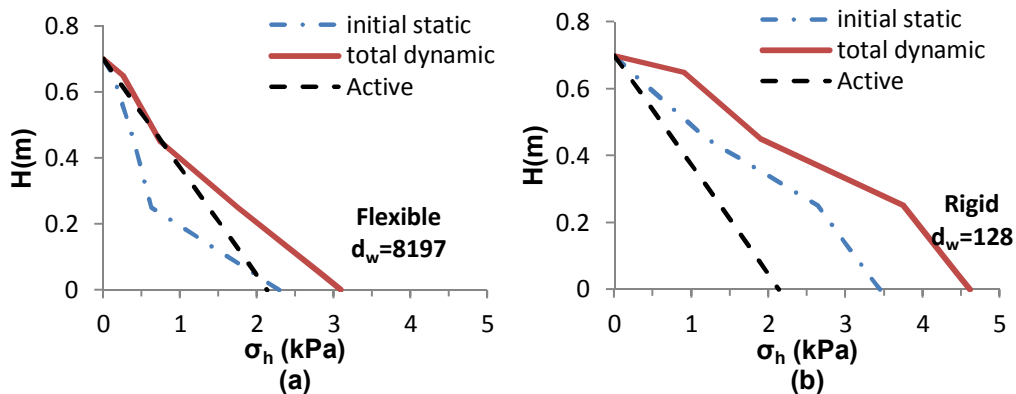


Figure 8 Pressure profiles along the wall stem (deformable buffer is not present)

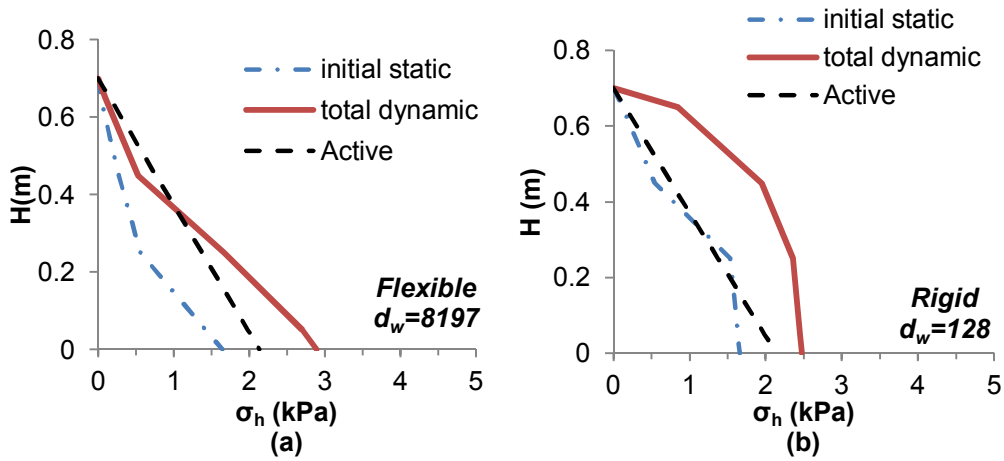


Figure 9 Pressure profiles along the wall stem (EPS-15 deformable buffer, $t/H=0.07$)

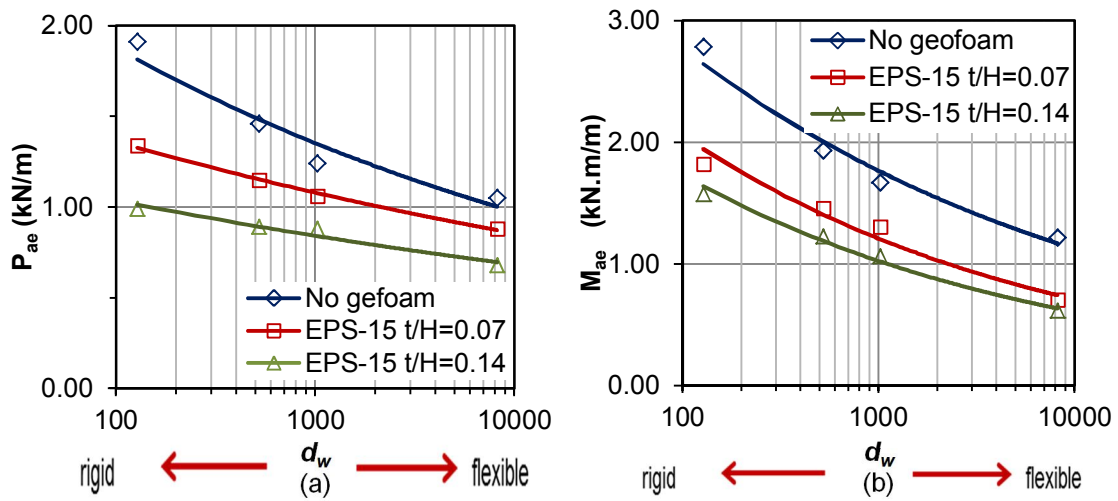


Figure 10 (a) Total dynamic wall thrust (P_{ae}) vs d_w (b) Bending moments (M_{ae}) vs d_w

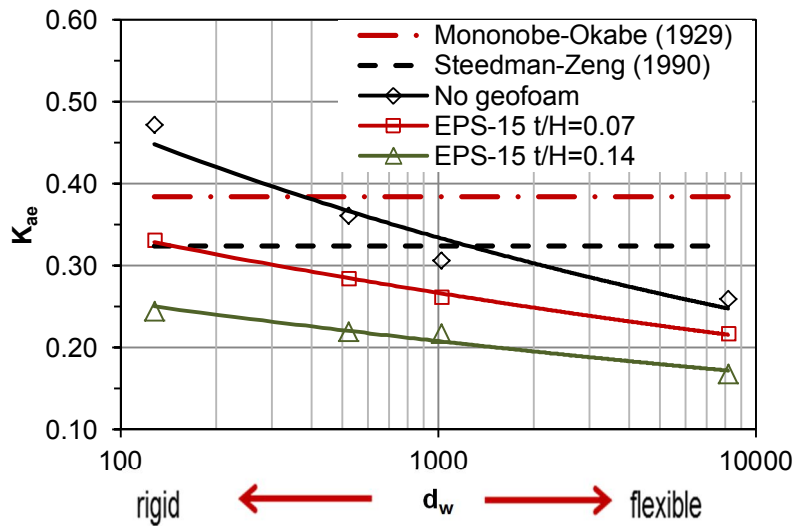


Figure 11 Variation of dynamic earth pressure coefficient (K_{ae}) with d_w ($f=4.25\text{Hz}$, $a_{\max}=0.3\text{g}$)

4. CONCLUSIONS

Results of this study demonstrate the positive role of geofoam buffers in improving the seismic performance of flexible retaining walls. The dynamic response of the model walls was evaluated in terms of flexural wall deflections and lateral earth pressures within the backfill. Dynamic earth pressure coefficients were calculated from the lateral stresses measured in the physical tests and compared with those calculated using methods available in the literature. It was observed that an increase in the relative wall flexibility provides reduction in the dynamic earth pressure coefficients. The presence of a deformable EPS geofoam buffer provides additional reduction in dynamic earth pressure coefficients for the investigated relative wall flexibility range. Dynamic earth pressure coefficients (K_{ae}) predicted by Mononobe-Okabe and Steedman-Zeng methods are in agreement with the test results for moderate relative flexibility values.

REFERENCES

- Horvath, J. S. (1997). Compressible inclusion function of EPS geofoam. *Geotextiles and Geomembranes*, **15**(1), 77-120.
- Ertuğrul, Ö. L., Trandafir, A. C. (2011). Reduction of Lateral Earth Forces Acting on Rigid Non-Yielding Retaining Walls by EPS Geofoam Inclusions. *ASCE Journal of Materials in Civil Engineering*. **23**(12): 1711-1718.
- Bathurst, R., Zarnani, S., Gaskin, A. (2007a). Shaking Table Testing of Geofoam Seismic Buffers. *Soil Dynamics and Earthquake Engineering*. **27**(4): 324-332.
- Athanasopoulos, G. A., Nikolopoulou, C. P., Xenaki, V. C. (2007). Reducing the seismic earth pressure on retaining walls by EPS geofoam-buffers-numerical parametric study. *Proceedings of the 2007 Geosynthetics Conference*. Vol I.
- Zarnani, S., Bathurst, J. (2009a). Numerical parametric study of expanded polystyrene geofoam seismic buffers. *Canadian Geotechnical Journal*. **46**: 318-338.
- Chang, N. Y., Makarechi, H. (1982). Effects of gradation on shear modulus of Denver sand at small strains. *Proceedings of the 1st International Conference on Soil Dynamics and Earthquake Engineering*. Vol. I: 117-129.
- Bathurst, R. J., Hatami, K. (1998). Seismic response analyses of a geosynthetic reinforced soil retaining wall. *Geosynthetics International*. **5**(1): 127-166.
- Iai, S. (1989). Similitude for shaking table tests on soil-structure-fluid model in 1-g gravitational field. *Soils and Foundations*. **29**:105-118.
- Okamoto M., F. S. (2006). Geomechanics and Geotechnics of Particulate Media. In M. Hyodo, An evaluation of the dry pluviation preparation technique applied to silica sand samples (pp. 33-39). London: Taylor and Francis Group.
- Younan, A. H., Veletsos, A. S. (2000). Dynamic response of flexible retaining walls. *Earthquake Engineering and Structural Dynamics*. **29**:1815-1844.